Design of Asynchronous STW Resonators for Filters and High Stability Source Applications

J.-M Friedt, S. Alzuaga, N. Ratier, N. Vercelloni, R. Boudot, B. Guichardaz, W. Daniau, V. Laude, S. Ballandras
FEMTO-ST, Dpt LPMO
32, avenue de l'Observatoire
25044 Besançon Cedex FRANCE
Email: jmfriedt@lpmo.edu

***Abstract*— We here investigate a new approach to creating high quality-factor resonators for filtering and oscillator applications based on STW wave propagation. We show that breaking the finger width periodicity, as opposed to the spacing between fingers, is an effective way of reducing spurious bulk modes and hence unwanted ripples out of the resonance frequency range. However, this improvement in terms of filtering applications comes with the drawback of a decreased quality factor which makes such devices unsuitable to oscillator applications. On the other hand, we conclude from simulations that narrow fingers in the transducers surrounded by wide fingers in the mirrors will lead to highest quality factors but increased losses. Experimental results at 750 MHz and 1.015 GHz are presented with loaded quality factors in the 5800-6700 range and are compared with a simplified mixed matrix based model.**

I. Introduction

Surface acoustic wave devices are used as resonator in stable oscillators for frequency source applications, as well as for filtering in ladder-type setups in the 900-2.5 GHz bands. In both cases spurious responses are to be eliminated since the spectral purity or transfer function of the resulting filter would be disturbed by such unwanted modes. Surface Transverse Waves (STW) display greater QF product (quality factor times frequency) than Rayleigh wave and will thus be the focus of this presentation.

The objective of this study is to evaluate a method for reducing spurious modes in surface acoustic wave resonators. We investigate the effect of modifying the metalization to electric period ratio (finger width to spacing ratio) on the propagation of STW resonators [1]–[3] as an alternative technique to reducing the conversion from surface to bulk acoustic waves which is conventionally obtained by changing the periodicity between the transducer and the Bragg mirrors around this transducer [4]. Hence we here keep the periodicity constant over the whole device and only modify the width of the fingers between the transducer and the mirrors.

The idea of modifying the finger width a to electrical period p (Fig. 1, bottom, for a definition of these values) ratio between the transducers and the mirrors stems from the observation that any periodicity breaking within an STW transducer strongly attenuates this acoustic mode. On the other hand the observation (Fig. 1) that keeping the periodicity of the electrodes in the transducer and mirror constant but varying the width of the electrodes leads to an improvement of the reflection efficiency of the mirrors if the latter display an a/p coefficient larger than that of the transducers hints at the possibility of an optimal set of finger widths in the transducer and the mirror.

Hence, we here investigate experimentally the validity of this hypothesis, and evaluate theoretically which set of a/p parameters in the transducer (as well as the cavity in the case of quadrupole resonators) and a/p in the mirrors leads to the best results in terms of quality coefficient for oscillator application, or least spurious modes for filter applications.

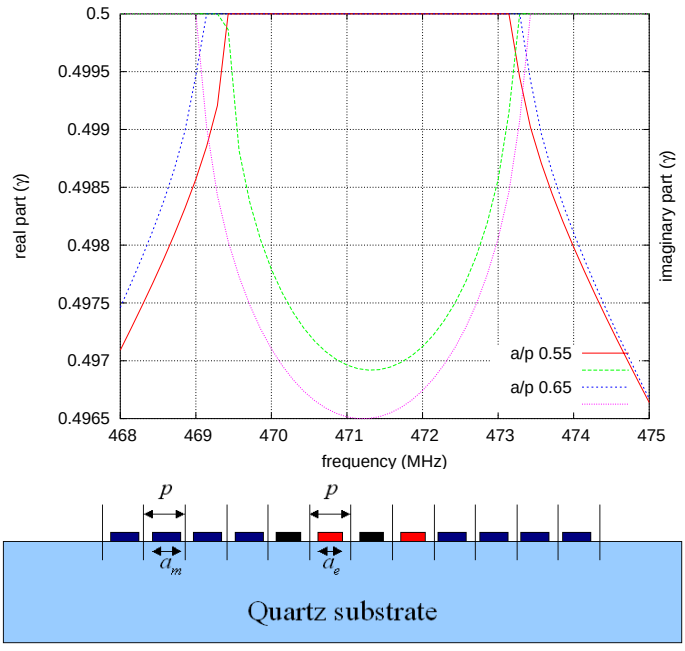

Fig. 1. Top: illustration of the evolution of real (red, blue) and imaginary (green, magenta) parts the wavevector as a function of the finger width to period ratio a/p. Notice that for a wider finger width to period ratio ($a/p = 0.65$) the stop band covers a wider frequency range meaning that the efficiency of mirrors patterned with such a geometry will have an improved reflection efficiency when working at frequencies compatible with the narrower stop band observed for $a/p = 0.55$ which is the geometry chosen for the transducers. Bottom: schematic of a cross section of the resonator displaying the constant periodicity p of the electrodes over the whole device and the varying electrode width a in the transducer and in the mirror.

The effects of metallic coating thickness during the elec-

trode deposition as well as the influence of varying the finger width to electrical period over the whole device are investigated (synchronous devices). Additionally, the original approach presented here to avoid unwanted surface-to-bulk mode conversion effects is to change the finger width between the transducers and the mirrors (asynchronous devices).

II. Fabrication procedures

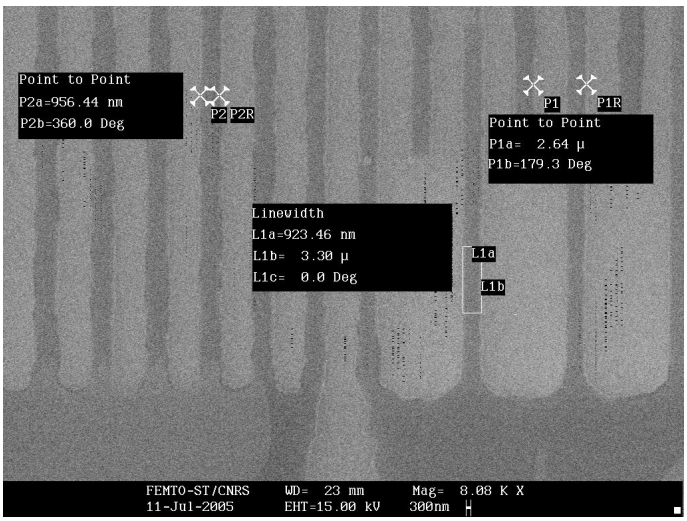

Fig. 2. Scanning electron microscope images of a synchronous device (the mirror is to the left of the image and the interdigitated transducer to the right).

Synchronous and asynchronous dipole and quadrupole resonators were processed in our class 10000 cleanroom. A 700 to 1000 Å thick aluminum layer – aluminum thickness being one of the variable parameters being investigated – was sputtered on 500 μm-thick AT-cut quartz wafers. Interdigitated transducers with electric periods of 2.5 μm and 3.38 μm were patterned, leading respectively to STW-mode surface acoustic waves propagating at a resonance frequency of about 750 MHz and 1.015 GHz.

Two sets of resonators were designed: dipoles and quadrupoles. In the former a single interdigitated transducer is surrounded by two patterned mirrors. In the latter a couple of interdigitated transducers and mirrors are located on both sides of a cavity. The spacing between successive fingers is always one quarter of the acoustic wavelength or one half of the electrical wavelength p, the latter being the measurement unit used throughout this discussion.

For each kind of transducer (dipoles and quadrupoles) two sets of devices were designed: synchronous and asynchronous (Fig. 2):

- **synchronous** devices display a constant finger width a to electric period p over the whole structure – mirror, transducer and cavity, the actual a/p value being a variable under investigation.
- **asynchronous** devices include a finger width variation in the finger width a between the mirror and the transducers while keeping the periodicity (spacing between the fingers) constant (Fig. 1, bottom). This approach contrasts with the more common design of changing the periodicity p between the transducers and the mirrors. In case of the quadrupoles, the periodicity and finger width in the cavity is always that of the surrounding transducers.

The measurements we made on the fabricated devices are

- in case of the quadrupoles, we measure the modulus of the transfer function S_{21} using a Rohde & Schwartz ZVC network analyzer, from which we extract the quality factor and visually estimate the relative height of the resonance peak to the sideband ripples,
- in case of the dipoles, we measure the admittance of the reflection coefficient Y_{11} and focus on the real part of this quantity to extract the quality factor and estimate the relative amplitude of the ripples to the main resonance peak.

III. Experimental results

Dipole resonators consist of a 150 finger-pairs transducer surrounded on both sides by 400 finger wide Bragg mirrors. Quadrupole resonators are designed with two 100 finger-pairs transducers, separated by a 10 finger wide cavity. The mirrors located on both sides of the transduction region are made of 400 fingers.

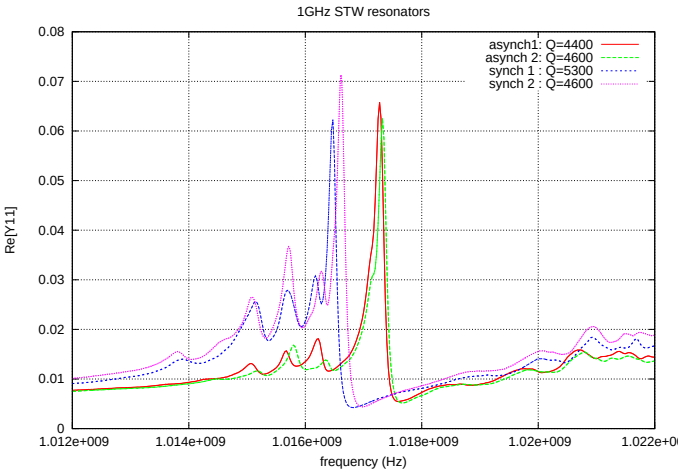

Fig. 3. Comparison of the measured admittance (real part) of synchronous and asynchronous two-port resonators. Although the asynchronous design displays less ripples out of the pass-band frequency range – making them suitable for narrow-band filtering applications – they display a lower quality factor than the synchronous design – making the latter more suitable for oscillator applications.

The reflected admittance $Y_{11}(f)$ for dipoles, and $S_{21}(f)$ transmission coefficient for the quadrupoles, are displayed in Figs. 3 (dipoles) and 4 (quadrupoles).

We observe that the asynchronous structures do not improve as was originally expected the quality factor as required for oscillator applications compared to the conventional synchronous designs. On the other hand the magnitude of the spurious modes out of the band pass frequency range are attenuated as required by narrow band filtering applications.

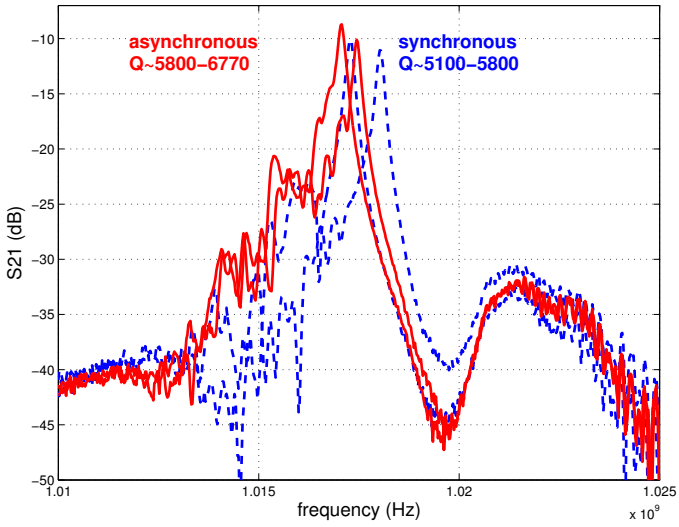

Fig. 4. Experimental measurement of quadrupole synchronous and asynchronous resonators insertion loss (magnitude of S_{21}).

IV. Models

The admittance of the synchronous and asynchronous devices have been simulated based on a simplified mixed matrix based model described in [5]–[7].

Let us consider an elementary cell of a periodic transducer (i.e. one period) still assuming infinite length of the electrode along x_3 as depicted in fig. 5.

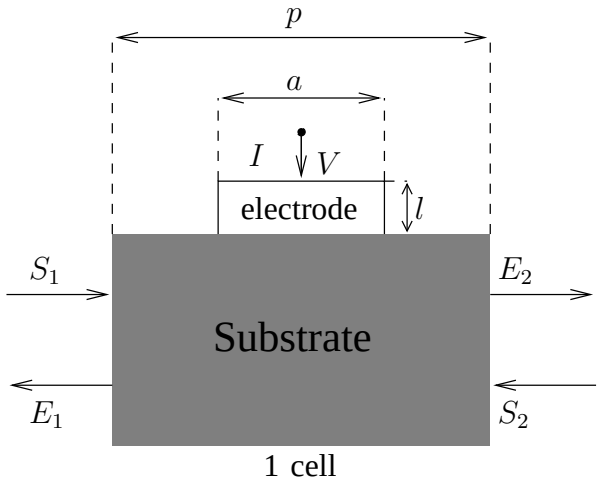

Fig. 5. Definition of the elementary cell of a mixed matrix model

The mixed matrix relates the outputs S of this elementary cells to it inputs E and describes the electro-acoustic couplings for a given mode of the structure. Using fundamental laws such as power preservation, reciprocity and the charge preservation, the simplified relationship is

$$\begin{pmatrix} S_1 \\ S_2 \\ I \end{pmatrix} = \begin{pmatrix} r_1 & t & \alpha_1 \\ t & r_2 & \alpha_2 \\ -\alpha_1 & -\alpha_2 & G+jB \end{pmatrix} \begin{pmatrix} E_1 \\ E_2 \\ V \end{pmatrix}$$

where coefficients r and t describe the acoustic diffraction phenomena observed from the cell boundaries (r and t respectively hold for reflection and transmission), α denotes the ability of the cell to convert electric signal into acoustic propagation (and vice versa), and $G + jB$ is its electrical admittance.

Note that reflection coefficients r from both sides of the cell as well as coupling parameters α are dissociated due to the possible existence of directivity properties of the substrate. As described in details in [6], it is possible to relate these coefficients to parameters extracted from harmonic admittance computations. Assuming no directivity in the cell, which corresponds to most of the crystal cuts used for RF devices, the following relations are used to define mixed matrix coefficients:

$$r_1 = r_2 = -j\sin(\Delta)\exp(-j\varphi)$$

$$t = \cos(\Delta)\exp(-j\varphi)$$

$$\alpha_1 = \alpha_2 = j\sqrt{G}\exp\left(-j\frac{\varphi+\Delta}{2}\right)$$

$$B = G\frac{\sin(\varphi)-\sin(\Delta)}{\cos(\Delta)-\cos(\varphi)}$$

Finally, one has to compute the coefficients Δ, φ and G in order to settle the electro-acoustic properties of one cell for the considered mode. As above-mentioned, these latter coefficients are deduced from harmonic admittance computations. Assuming f_s and f_e as the edge of the frequency stop band and y_s and y_e the corresponding magnitude of the harmonic admittance, one can derive [6], [7] the following relations:

$$|\Delta| = \pi\frac{f_e - f_s}{f_e + f_s}\ ;\varphi = 2\pi\frac{f}{f_e + f_s}\ ;G = \frac{y_s - y_e}{\tan(|\Delta|)}$$

It is then easy to chain mixed matrices one to the others in order to simulate a device exhibiting a given number of periods (the so-called cells) assuming proper boundary conditions at the edges of the gratings and taking into account the static capacitance of the structure. However, the simulation of acoustic radiation from the surface to the bulk of the substrate is not taken into account rigorously using mixed matrix. The use of empirical formulas for given devices can give access to the contribution of radiated bulk waves to the electrical admittance but the rigorous simulation of these phenomena using the mixed matrix approach remains an open problem. Here the propagation of bulk modes is thus not included in the simulation results.

V. Results and Discussion

Modeling displays an obvious dependence of the quality factor with a/p ratio. For example for a synchronous dipole structure with 750 nm thick aluminum layer patterned for describing the interdigitated transducer and mirror structures, a sharp quality factor optimum is displayed for $a/p = 0.7$ (simulation data not shown). The strong dependence of the

resulting resonant frequency and peak sharpness to the a/p ratio hints at the experimental difficulties met when making these actual sensors for high frequency (>1 GHz) applications for which the electrical period is already as low as 2.5 μm, this requiring a processing lateral-accuracy during the lithography step the 100 nm, beyond what we can reach in a general purpose clean room (Fig. 2).

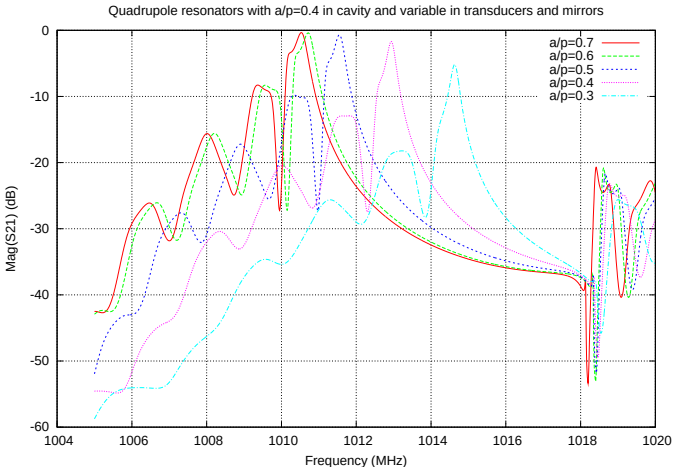

Fig. 6. Simulations of the response of STW quadrupole resonators in which the a/p ratio is kept constant over the mirror and transducers but varied in the cavity region (5 finger pairs). We notice that the cavity hardly affects the shape of the response which is thus representative of the synchronous device configuration.

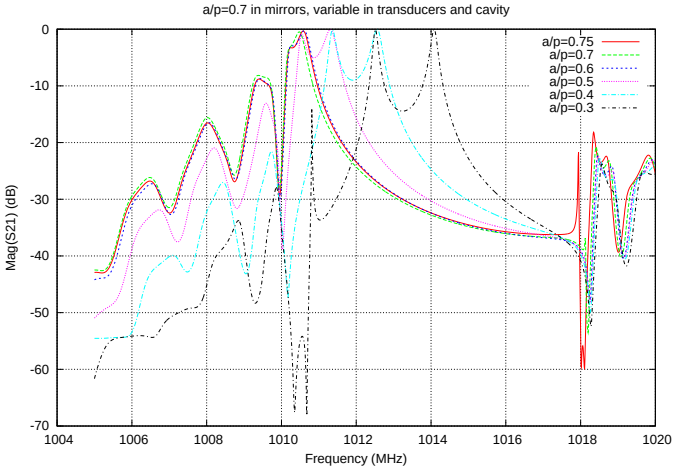

Fig. 7. Simulations of the response of STW quadrupole resonators in which the a/p ratio is kept equal to 0.7 in the mirrors and varied in the transducer and cavity.

Fig. 6, which displays the simulation of the transfer function $|S_{21}|$ of a quadrupole resonator, leads us to predict that a lower a/p over the whole synchronous device increases the quality factor but also increases the insertion loss. Additionally, spurious modes below the resonance frequency become predominant in the shape of the transfer function for greater a/p ratio. It thus seems that lower values of a/p lead to the best responses both for filtering applications (in which spurious modes are to be avoided) and frequency sources (highest quality factor).

We then consider Fig. 7 in which the a/p ratio is kept constant and equal to 0.7 in the mirrors and the finger width is varied in the transducers and the cavity. Here again we are thus simulating the response of quadrupoles, but this time in an asynchronous configuration. We here clearly observe that the lower the a/p ratio in the transducer and the cavity, the sharper the resonance and hence the greater the quality factor – as expected from an improved efficiency of the mirrors as the a/p ratio in the mirrors greatly differs from that same ratio value in the transducers – but additionally that a second mode appears below the resonance frequency. This two modes degenerate in a single wider mode (lower quality factor) as the a/p ratio in the transducers becomes closer to this ration in the mirrors.

VI. Conclusion

We have modelled and fabricated synchronous and asynchronous STW resonators in dipole and quadrupole configurations. We observe that

- sideband ripples are strongly attenuated in the asynchronous design, making such designs suitable for filtering applications,
- the quality factor is either not affected or slightly degraded in the asynchronous design compared to the results observed with synchronous devices, making the latter best suited for frequency source application.

Having validated the models with experimental data within uncertainties associated to the fabrication process, we can now consider a systematic search for an optimum configuration of the finger width in the mirror and the transducers depending on the requirements of the device to be designed.

Acknowledgment

This work was supported by the French Direction Générale de l'Armement (DGA) under grant number 04-34-029-00-470-75-65. We are grateful to T. Pasturaud (TEMEX, France) for fruitful discussions and assistance in modeling.

References

[1] A. Auld, J. Gagnepain, and M. Tan, "Horizontal shear surface waves on corrugated surfaces," *Electron. Lett.*, vol. 12, pp. 650–652, 1976.

[2] V. Gulyaev and V. P. Plessky, *Sov. Tech. Phys. Lett.*, vol. 3, pp. 87–88, 1977.

[3] I. D.Avramov, "High-performance surface transverse wave resonators in the lower GHz frequency range," *Internatioal Journal of High Speed Electronics and Systems*, vol. 10, pp. 735–792, 2000.

[4] P. Wright, "A review of saw resonator filter technology," in *Ultrasonics Symposium*, 1992, pp. 29–38.

[5] S. Ballandras, T. Pasturaud, V. Laude, W. Steichen, W. Daniau, R. Lardat, M. Solal, J. Briot, S. Chamaly, M. Doisy, X. Perois, and P. Girard, "Ferroelectric materials for modern surface acoustic wave devices," *Piezoelectric Materials for Macro/Micro Systems*, pp. 183–197, 2003.

[6] J. Hodé, J. Desbois, P. Dufilié, M. Solal, and P. Ventura, "Spudt-based filters : Design principles and optimization," in *Proc. of the IEEE Ultrasonics Symp.*, 1995, pp. 39–50.

[7] P. Ventura, J. Hodé, M. Solal, J. Desbois, and J. Ribbe, "Numerical methods for saw propagation characterization," in *Proc. of the IEEE Ultrasonics Symp.*, 1998, pp. 175–186.